# Analysis of invariant spanning curves in oval billiards: A numerical approach based on Slater's theorem ⊘

Joelson D. V. Hermes 🗷 🗓 ; Matheus Hansen 🗓 ; Sishu S. Muni 🗓 ; Edson D. Leonel 🗓 ; Iberê Luiz Caldas 🗓



Chaos 35, 033132 (2025)

https://doi.org/10.1063/5.0250725





# Articles You May Be Interested In

Dynamics of classical particles in oval or elliptic billiards with a dispersing mechanism

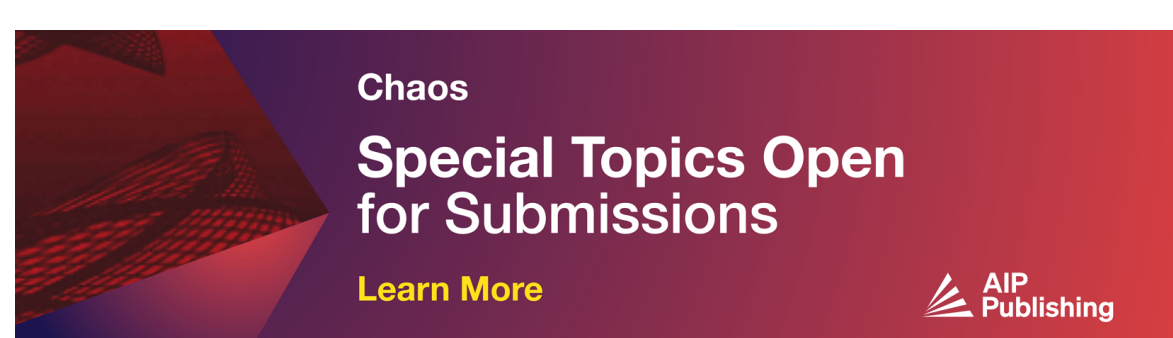
Chaos (March 2015)

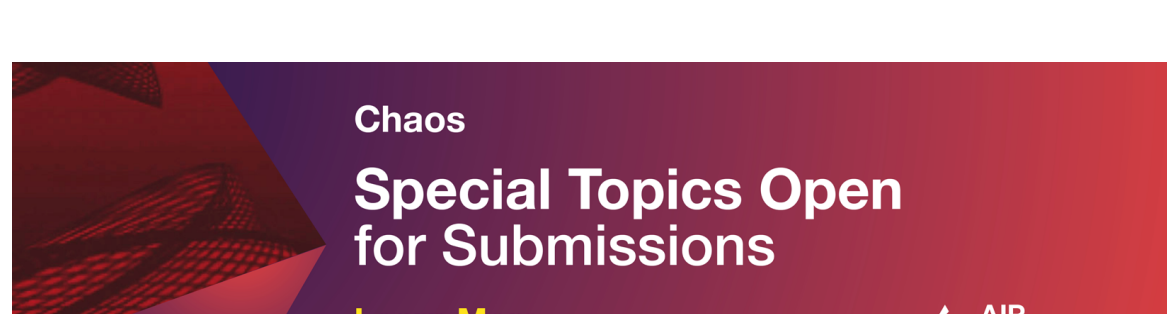
Fermi acceleration and scaling properties of a time dependent oval billiard

Chaos (September 2009)

Dynamical thermalization in time-dependent billiards

Chaos (October 2019)







14 March 2025 17:24:15



# Analysis of invariant spanning curves in oval billiards: A numerical approach based on Slater's theorem

Cite as: Chaos 35, 033132 (2025); doi: 10.1063/5.0250725 Submitted: 26 November 2024 · Accepted: 1 March 2025 · Published Online: 14 March 2025







Joelson D. V. Hermes, 1,2,a) D Matheus Hansen, D Sishu S. Muni, D Edson D. Leonel, D and Iberê Luiz Caldas D

# **AFFILIATIONS**

- <sup>1</sup>Federal Institute of Education, Science and Technology of South of Minas Gerais—IFSULDEMINAS, 37576-000 Inconfidentes,
- <sup>2</sup>Physics Institute, University of São Paulo—USP, 05508-090 São Paulo, SP, Brazil
- <sup>3</sup>Center for Mathematics and Applications (NOVA Math), NOVA School of Science and Technology, Universidade NOVA de Lisboa, Quinta da Torre, 2829-516 Caparica, Portugal
- <sup>4</sup>School of Digital Sciences, Digital University Kerala, Pallipuram 695317, Kerala, India
- Department of Physics, São Paulo State University—UNESP, 13506-900 Rio Claro, SP, Brazil

#### **ABSTRACT**

The study of billiards investigates the trajectories of particles that move freely in a region and reflect elastically at boundaries. Although there is already considerable understanding about invariant spanning curves, also known as whispering gallery orbits in the context of billiards, their determination in the phase space of the system, in addition to the analysis of their existence is still an open question. Our proposal is to present a numerical method based on Slater's theorem, capable of determining the location of these curves in phase space, as well as finding the critical parameter at which these curves are no longer observed. In this work, we apply this method to determine the location of a set of invariant spanning curves in an oval billiard for different parameter values. Furthermore, we identified the critical parameter at which the phase space no longer presents these curves and local chaos becomes global. We compared our numerical results with analytical results present in the literature, proving the effectiveness of the proposed method. By studying the rotation number, we obtain additional information about the behavior of these curves and also of the systems.

Published under an exclusive license by AIP Publishing. https://doi.org/10.1063/5.0250725

In this paper, we present a numerical method based on Slater's theorem to investigate invariant curves in oval billiards, addressing a challenge that remained without clear evidence in the literature: the precise location of these curves in phase space and the determination of the critical parameter  $\varepsilon_c$  at which they are destroyed. Although previous studies have predicted the destruction of these curves, concrete evidence to validate these predictions has not yet been provided. The proposed method combines high accuracy with computational efficiency, revealing the position of the curves and confirming the validity of the theoretical predictions. Furthermore, the analysis of the rotation number provides details on the transition dynamics between periodic and chaotic regions in phase space. This work not only fills important gaps in the understanding of billiard dynamics but also offers a robust tool for the analysis of invariant structures and their implications in nonlinear dynamical systems.

# I. INTRODUCTION

The dynamics of billiards have proven to be a captivating field of study, providing valuable perceptions not only for the theory of dynamic systems but also for numerous practical applications. The investigation of these systems offers a unique perspective on the complexity of particle trajectories interacting with rigid boundaries, presenting intriguing challenges and motivating further exploration.

Billiards, as idealized systems of particles reflecting off boundaries, 1,2 play a crucial role across various domains, from fundamental physics to practical problem-solving applications. They serve as simplified models to comprehend complex phenomena, finding widespread applications in areas such as optics,3 acoustics,4 superconducting,5 and studies involving mesoscopic quantum dots.6

Within the realm of billiards, invariant curves emerge as fundamental elements.<sup>7,8</sup> These curves, which remain unchanged over

a) Author to whom correspondence should be addressed: joelson.hermes@ifsuldeminas.edu.br

time, play a vital role in characterizing and understanding the overall behavior of the system. In particular, invariant spanning curves are crucial in separating regions with different dynamical behaviors, serving as barriers that confine trajectories and prevent the global diffusion of phase space. They dictate a scaling property that leads to critical exponents analogous to those observed in phase transitions. Their significance extends beyond billiards, as they are fundamental structures in nonlinear dynamical systems, including Hamiltonian systems, plasma confinement, of and celestial mechanics. The presence or destruction of these curves directly influences the long-term stability of a system, impacting the predictability and transport properties of dynamical trajectories.

Specifically, determining invariant curves in oval billiards represents a significant and essential challenge to elucidate the complexity of these systems. Previous studies have substantially contributed to understanding billiards, showcasing important discoveries such as the expression for the critical parameter for global chaos. <sup>12</sup> However, despite these advances, a crucial aspect remains unexplored: the precise determination of the positions of invariant curves. Our work aims to fill this gap, providing an innovative approach that allows for the accurate determination of these curves in oval billiards.

Furthermore, our study incorporates Slater's theorem, <sup>13,14</sup> a fundamental result in the theory of dynamic systems, stating that in a quasiperiodic orbit, there are at most three recurrence times, with the largest being equal to the sum of the other two. This theory plays a crucial role in our work, providing a solid theoretical framework for the analysis of invariant curves in oval billiards.

Thus, the relevance of this study extends beyond the mere determination of invariant curves in oval billiards; it contributes to advancing the understanding of complex dynamic systems and applying this knowledge in various fields. We hope that this work not only addresses gaps in existing knowledge but also inspires future research, contributing to the continuous development of the theory of dynamic systems and its practical applications.

This paper is organized as follows: in Sec. II, we present the billiard model used in this study, describing its properties. In Sec. III, we detail the method based on Slater's theorem, explaining its application in determining invariant spanning curves. In Sec. IV, we show the results obtained through the application of this method, highlighting the location of the curves in phase space, the determination of the critical parameter and comparing them with the results present in the literature. In Sec. V, we perform a rotation number analysis, providing an additional understanding of the behavior of invariant spanning curves. Finally, in Sec. VI, we present our final considerations, summarizing the main conclusions.

#### II. THE MODEL

The dynamics of a billiard essentially consist of the evolving of a classical particle in a closed region delimited by a rigid boundary, with which the particle collides and is reflected specularly (the incidence angle at the collision point is equal to the reflected one). When the boundary is assumed as static over time and the collisions are of the elastic type, the particle experiences the conservation of its energy throughout the entire evolution of dynamics.<sup>12</sup>

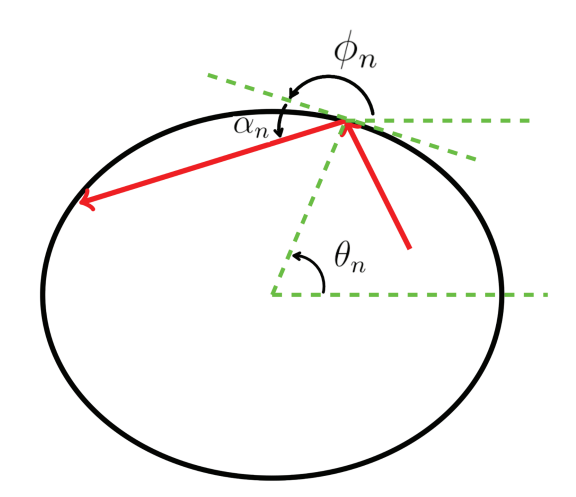


FIG. 1. Schematic draft for a collision (red line) of a particle in an oval billiard.

If we assume a generic billiard with a static boundary described in the polar form by  $R_b(\theta)$ , then it is possible to describe the particle dynamics for the nth collision inside of the system through the angular variables  $(\theta_n, \alpha_n)$ , where the dynamical variable  $\theta_n$  represents the position of the particle along the boundary and  $\alpha_n$  indicates the angle formed by the trajectory of the particle and a tangent line to the boundary at position  $\theta_n$  (see Fig. 1). Assuming the absence of potential acting within the billiard and a scenario of elastic collisions, the particle will then exhibit a motion with a constant velocity (in magnitude) along a straight line between the collisions in the system (free motion). In such case, we can write the radial position of the particle at time t inside the billiard as

$$R_p(t) = \sqrt{X_p^2(t) + Y_p^2(t)},$$
 (1)

where  $X_p(t)$  and  $Y_p(t)$  are, respectively, the rectangular coordinates of the particle, i.e.,

$$X_p(t) = X(\theta_n) + |\vec{V}_n| \cos(\alpha_n + \phi_n)[t - t_n], \tag{2}$$

$$Y_p(t) = Y(\theta_n) + |\vec{V}_n|\sin(\alpha_n + \phi_n)[t - t_n], \tag{3}$$

with  $|\vec{V}_n|$  indicating the speed of the particle and  $\phi_n = \arctan\left[\frac{Y'(\theta_n)}{X'(\theta_n)}\right]$ , where  $X'(\theta_n) = dX(\theta_n)/d\theta_n$  and  $Y'(\theta_n) = dY(\theta_n)/d\theta_n$ .

Numerically, we define a new collision  $\theta_{n+1}$  of the particle with the boundary solving the implicit equation  $R_p(\theta_{n+1}, t_{n+1}) = R_b(\theta_{n+1})$ , with time  $t_{n+1}$  given by

$$t_{n+1} = t_n + \frac{\sqrt{\Delta X_p^2 + \Delta Y_p^2}}{|\vec{V}_n|},$$
 (4)

where  $\Delta X_p = X_p(\theta_{n+1}, t_{n+1}) - X(\theta_n)$  and  $\Delta Y_p = Y_p(\theta_{n+1}, t_{n+1}) - Y(\theta_n)$ .

Through the conservation of the momentum, we can find the reflection laws for the collision of the particle with the boundary. Taking into account that the billiard in the presented formalism

exhibits a static shape over time, then the velocity of the particle after the n+1 collision can be described along the tangent and normal components as

$$\vec{V}_{n+1} \cdot \vec{T}_{n+1} = \vec{V}_n \cdot \vec{T}_{n+1},\tag{5}$$

$$\vec{V}_{n+1} \cdot \vec{N}_{n+1} = -\vec{V}_n \cdot \vec{N}_{n+1},\tag{6}$$

where  $\vec{T}_{n+1} = \cos(\phi_{n+1})\hat{i} + \sin(\phi_{n+1})\hat{j}$  and  $\vec{N}_{n+1} = -\sin(\phi_{n+1})\hat{i} + \cos(\phi_{n+1})\hat{j}$  are, respectively, the tangent and normal unit vectors.

Naturally, the velocity of the particle in magnitude after the n + 1 collision is given by

$$|\vec{V}_{n+1}| = \sqrt{\left[\vec{V}_{n+1} \cdot \vec{T}_{n+1}\right]^2 + \left[\vec{V}_{n+1} \cdot \vec{N}_{n+1}\right]^2},$$
 (7)

while the reflection angle  $\alpha_{n+1}$  is

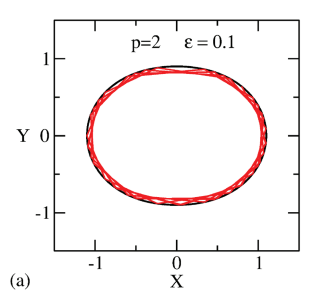
$$\alpha_{n+1} = \arctan \left[ \frac{\vec{V}_{n+1} \cdot \vec{N}_{n+1}}{\vec{V}_{n+1} \cdot \vec{T}_{n+1}} \right]. \tag{8}$$

As already known, the dynamic exhibited by a particle in a billiard is totally connected with the shape of the system, i.e., depending on the geometry of the boundary, the billiard might present different types of structures, such as integrable, <sup>12,15</sup> ergodic, <sup>16,17</sup> or mixed. <sup>18,19</sup> The last case can be considered the richest one for billiards, once from a dynamic point of view the phase space for the mixed case might present the coexistence of stability islands and invariant spanning curves that delimit regions of chaos. In this work, the model we will address is known as the oval billiard, <sup>12,20,21</sup> which falls under the mixed-type structure. The boundary of this billiard is described in polar coordinates by the equation

$$R(\theta, \varepsilon, p) = 1 + \varepsilon \cos(p\theta),$$
 (9)

where  $\varepsilon$  is the nonlinearity parameter corresponding to the perturbation amplitude of the circle. For  $\varepsilon = 0$ , we recover the circular billiard, which is integrable. On the other hand, if  $\varepsilon \neq 0$ , the phase space exhibits regular regimes, invariant curves, and chaos. The parameter p controls the deformation of the boundary, which is a positive integer value. Such parameters play a crucial role in billiard dynamics, since, depending on the combination of the  $\varepsilon$  and p parameters, the billiard boundary can be concave or convex. Furthermore, the concavity of the border is directly related to invariant spanning curves (whispering gallery orbits), which can be defined as a set of quasi-periodic curves that continue bordering along the billiard wall. A border with concave curvature ends up favoring orbits with these characteristics, as exemplified in Fig. 2(a). However, for a convex boundary, as shown in Fig. 2(b), the curvature of the wall itself prevents the particles from maintaining trajectories that go around the entire billiard wall, resulting in the extinction of this type of orbit that borders the boundary of the billiard. Thus, when the billiard boundary has a concave (positive) curvature, invariant spanning curves are observed, on the other hand, if the border is convex (negative), there are no curves of this type.

Due to the significant influence of the parameters  $\varepsilon$  and p on the dynamics of the system, works such as Ref. 12 were dedicated to finding an expression that relates these parameters and determines



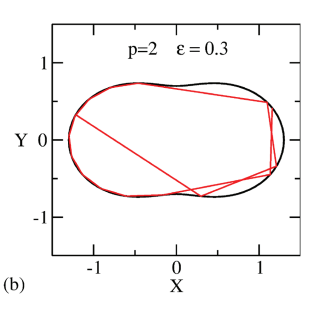


**FIG. 2.** Representation of a particular trajectory for two distinct boundaries: (a) p=2 and  $\varepsilon=0.1$  that corresponds to a concave boundary and (b) p=2 and  $\varepsilon=0.3$  that corresponds to a convex boundary.

the critical value of  $\varepsilon$  from which invariant spanning curves. This expression is given by

$$\varepsilon_c = \frac{1}{1 + p^2}, \quad p \ge 1, \tag{10}$$

where, for values of  $\varepsilon$  smaller than  $\varepsilon_c$ , the boundary becomes concave, while for values greater than  $\varepsilon_c$ , the concavity of the boundary is convex. Illustrating this situation, we have Fig. 3(a), where  $\varepsilon=0.1$  and p=2. We observe that according to Eq. (10),  $\varepsilon_c=0.2$ . Therefore, in this case,  $\varepsilon<\varepsilon_c$ , and in the phase space shown in Fig. 3(a), it is possible to notice the presence of invariant spanning curves, located in both the lower and upper parts of the phase space. Furthermore, we highlight in red the orbit shown in Fig. 3(a), confirming that this trajectory corresponds to a whispering gallery orbit, that is, to an invariant spanning curve. On the other hand, in Fig. 3(b), we have the phase space for  $\varepsilon=0.3$  and p=2, that is,  $\varepsilon>\varepsilon_c$ . In this case, it is possible to notice the absence of invariant spanning curves, and the chaos that was local in Fig. 3(a) becomes global, see Fig. 3(b).

In Sec. III, we will present a numerical method capable of determining the critical value of  $\varepsilon$  with good precision and also accurately determining the location of the invariant spanning curves in the phase space.

#### III. THE METHOD

Many studies have been dedicated to investigating invariant spanning curves in various models of dynamical systems, since these curves play a crucial role in the dynamics of these systems, acting as barriers in the process of particle diffusion and transport, delimiting the sea of chaos. However, in the context of billiards, there is a considerable gap, especially with regard to the location of these curves in phase space.

A notable work in this area is the study conducted by Oliveira *et al.*, <sup>12</sup> in which the authors managed to determine the critical parameter at which all invariant curves are destroyed. They exploited the concavity of the boundary to obtain such a result. However, this work focuses mainly on the behavior of the last curve, in addition to presenting a complex mathematical approach that requires laborious development. Moreover, their results provide an

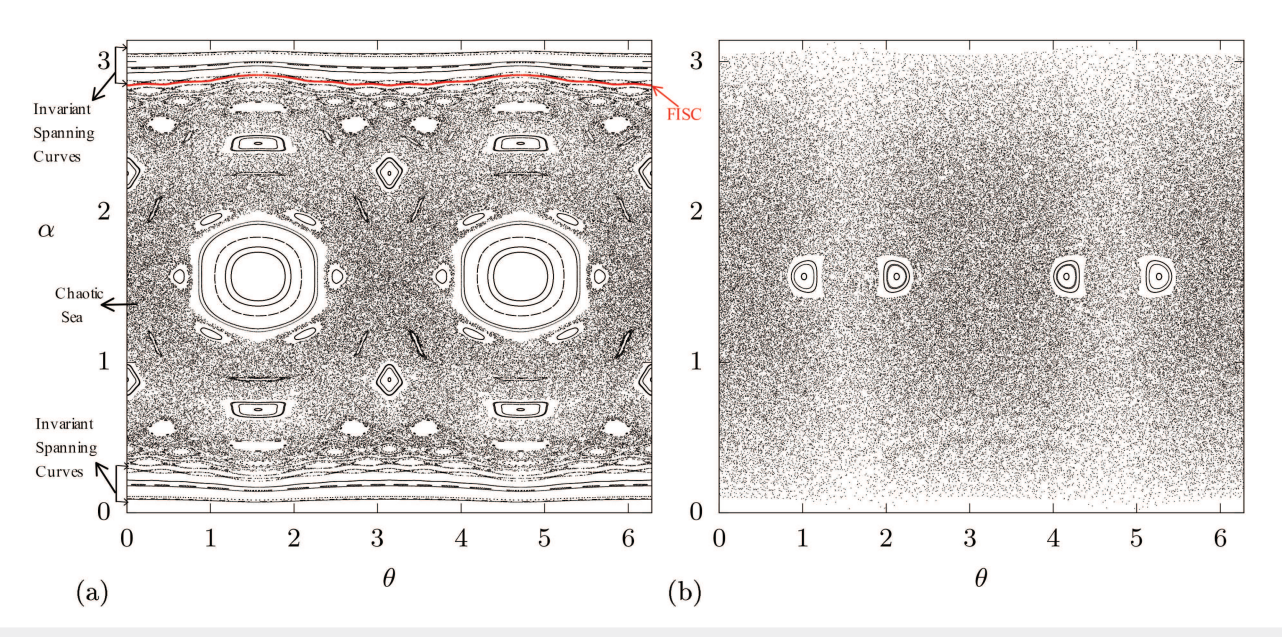


**FIG. 3.** Phase space for the oval billiard for p=2 and different values of  $\varepsilon$ . (a)  $\varepsilon=0.1$  and the red curve corresponds to the orbit highlighted in Fig. 2(a), this curve corresponds to the First Invariant Spanning Curve (FISC). (b)  $\varepsilon=0.3$  where all invariant spanning curves have been destroyed.

estimate for the critical parameter but do not include numerical verification. In our work, we aim to complement this analysis by providing numerical evidence to confirm the destruction of invariant curves, reinforcing the validity of their theoretical predictions.

Our proposal aims to utilize Slater's theorem<sup>13</sup> to identify multiple invariant curves within the phase space of an oval billiard. The implementation of the method is relatively straightforward, boasting a low computational cost when compared to alternative techniques. Nevertheless, this approach enables precise localization of these curves within the phase space. Additionally, it facilitates the determination of the critical parameter value associated with the destruction of the last curve. This method has previously demonstrated success in applications to the Standard Map,<sup>22</sup> Fermi–Ulam model,<sup>23</sup> and a family of Hamiltonian maps.<sup>24</sup> Such successful applications underscore the method's reliability and accuracy.

Slater's theorem<sup>13</sup> states that, for any interval of size  $\delta$  of a quasi-periodic trajectory, there are at most three different recurrence times:  $\Gamma_1$ ,  $\Gamma_2$ , and  $\Gamma_3 = \Gamma_1 + \Gamma_2$ . In other words, for an invariant curve with an irrational rotation number, only three recurrence times are observable, the largest of which is equal to the sum of the other two. To illustrate, consider a point moving along a circle with an irrational rotation number (e.g.,  $\sqrt{2}$  module 1). If we mark a small interval on the circle and track when the point revisits it, we will find that the time intervals between successive visits are constrained to exactly three distinct values, obeying  $\Gamma_3 = \Gamma_1 + \Gamma_2$ .

Applying the method involves checking whether or not a coordinate  $(\theta,\alpha)$  belongs to the invariant curve, which is done by checking whether there are only three recurrence times. Thus, for each pair  $(\theta,\alpha)$ , we apply Slater's theorem, calculating the number of iterations that an orbit takes to return to an interval  $\delta$  close to where it started. If there are only three distinct times, as predicted by Slater's

theorem, we conclude that the point  $(\theta, \alpha)$  belongs to an invariant curve. Otherwise, we advance one step  $\Delta\alpha$  in variable  $\alpha$  and repeat the procedure until the theorem is satisfied, identifying the point  $(\theta, \alpha)$  for which the condition was met as belonging to an invariant spanning curve.

Now, to determine the critical parameter  $\varepsilon_c$  after which all curves are destroyed, we proceed by gradually increasing the parameter  $\varepsilon$  and searching for invariant curves. Whenever we identify a coordinate  $(\theta, \alpha)$  that satisfies Slater's criterion, this indicates the presence of at least one invariant curve. Thus, when going through the entire range of phase space and not finding a pair  $(\theta, \alpha)$  that satisfies Slater's criterion, we conclude that all curves have been destroyed. The last value of  $\varepsilon$  for which we still identify some curve is then considered the critical parameter  $\varepsilon_c$ . In Sec. IV, we will present some results from the implementation of this method.

## **IV. NUMERICAL RESULTS**

Based on the methodology presented in Sec. III, we determined a set of invariant curves that satisfy Slater's theorem. Four of these curves are highlighted in Fig. 4, which represents the upper part of the phase space, showing the locations of the invariant curves. It is important to note that there are many invariant curves in this region, and the four highlighted are provided only as representative examples. In Table I, each of these curves is identified, along with the recurrence times corresponding to each one, confirming that all satisfy Slater's theorem, with the largest recurrence time equal to the sum of the other two. Furthermore, the table provides the initial coordinates  $(\theta,\alpha)$  analyzed and associated with each curve, allowing for the precise location of each curve on the graph in Fig. 4.

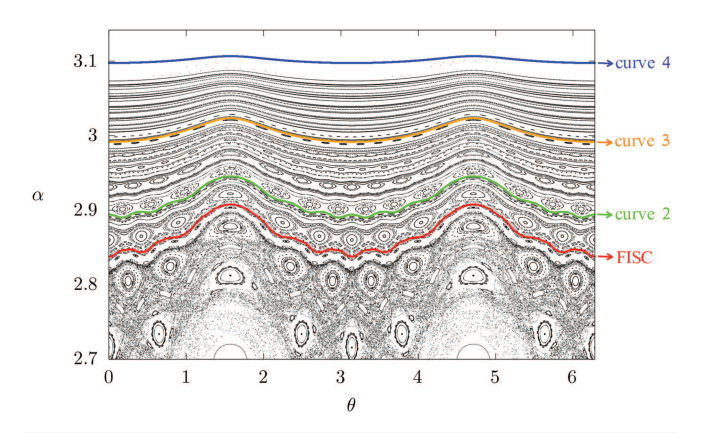


**FIG. 4.** Enlargement of the upper region of the phase space for p=2 and  $\varepsilon=0.1$ . The highlighted curves correspond to the curves found using the Slater criterion whose information is found in Table I.

Using this technique, we can identify specific curves, such as the First Invariant Spanning Curve (FISC). This curve plays a crucial role, since the critical exponents, which describe the transition from integrability to non-integrability in a two-dimensional nonlinear map, are obtained by locating the first invariant spanning curve in phase space. In a general class of systems, the position of the first invariant spanning curve is estimated by reducing the system mapping to the standard mapping, where there is a transition from local chaos to global chaos. However, this procedure is not

**TABLE I.** Recurrence times for  $\delta = 10^{-4}$  and coordinates for identified invariant spanning curves in Fig. 4.

	$\Gamma_1$	$\Gamma_2$	$\Gamma_3$	$(\theta, \alpha)$
Curve 4	14718	2059	16 777	$(\pi, 3.0974)$
Curve 3	5815	6511	12 326	$(\pi, 2.9914)$
Curve 2	12 356	7419	19 775	$(\pi, 2.8943)$
FISC	5205	9713	14 918	$(\pi, 2.8378)$

viable for billiards, as it would lead to the resolution of transcendental equations. However, when using Slater's theorem, determining this curve becomes feasible and highly accurate. This curve is highlighted in red (FISC) in Fig. 4. It is possible to observe the presence of a chain of islands both above and below the curve, with a vast sea of chaos being bounded by the first curve. Therefore, an initial condition given below the curve cannot penetrate the region of stability above it, just as an initial condition given above the curve never visits the chaotic region below it. These results illustrate the significant influence of the first invariant curve on the dynamic of systems, highlighting its importance in understanding the transition between different dynamic regimes.

As mentioned, the proposed method determines the critical parameter at which the last invariant spanning curve is destroyed, marking the point beyond which no spanning curve is observed in the system. We apply this analysis to the proposed billiards, starting with p=2. According to Eq. (10), for p=2,  $\varepsilon_c=0.2$ . Using our method, based on Slater's theorem, we found  $\varepsilon_c=0.195\,777\,2$ ,

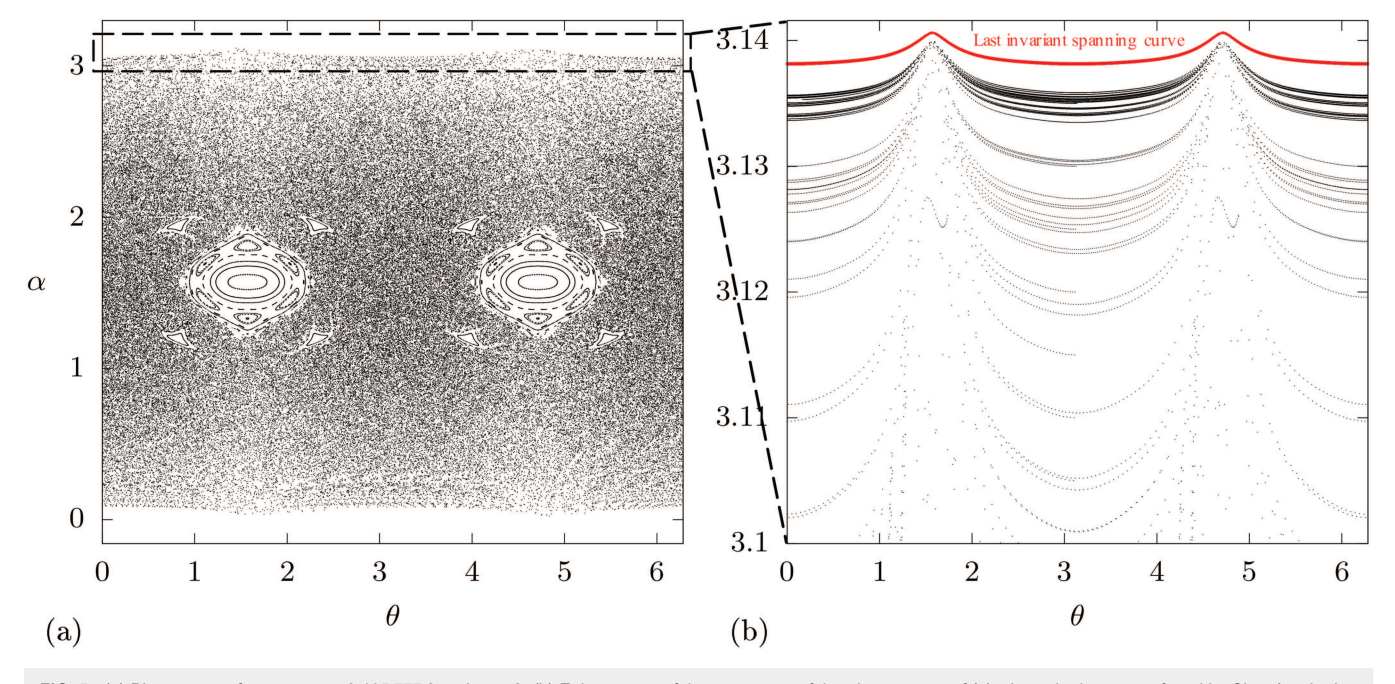


**FIG. 5.** (a) Phase space for  $\varepsilon = \varepsilon_c = 0.195\,777\,2$  and p = 2. (b) Enlargement of the upper part of the phase space of (a) where the last curve found by Slater's criterion is highlighted in red.

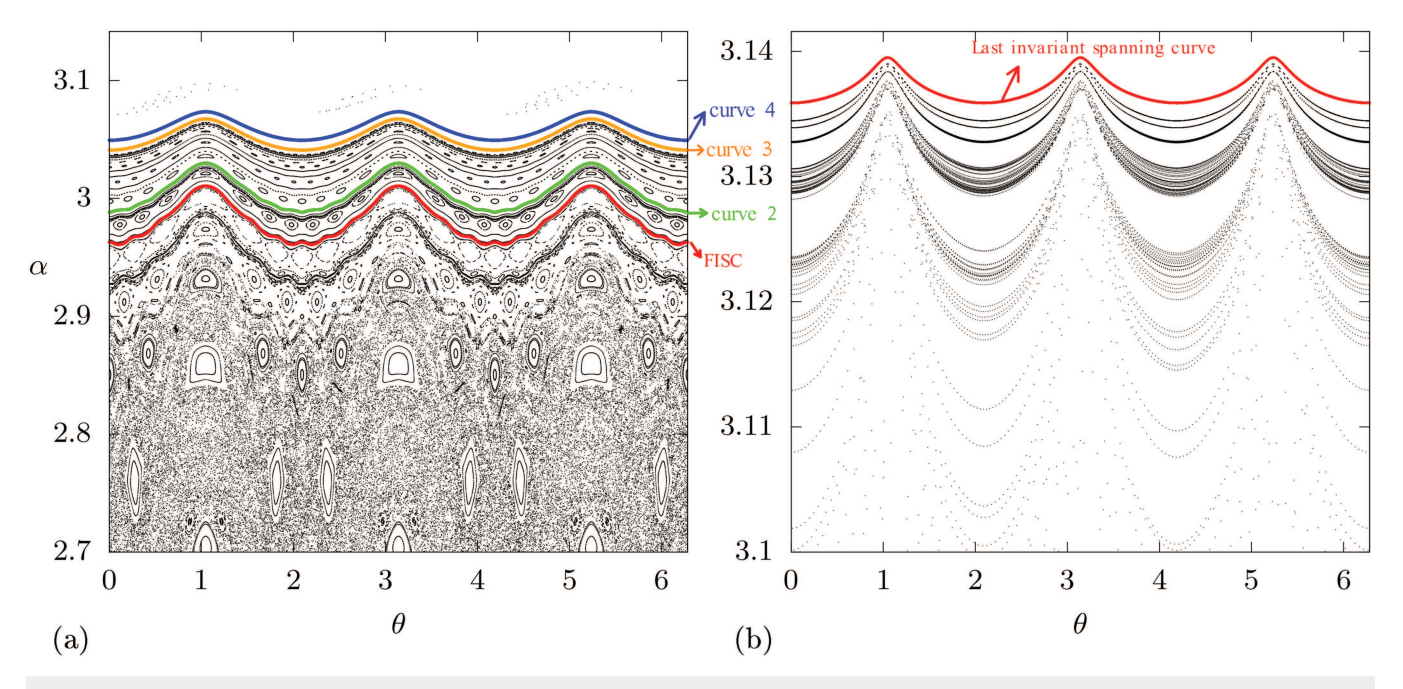


**FIG. 6.** (a) Phase space for  $\varepsilon=0.05$  and p=3, where the First Invariant Spanning Curve (FISC) and three other curves are represented. (b) Enlargement of the upper part of the phase space for  $\varepsilon=\varepsilon_c=0.195\,777\,2$  and p=3, where the last curve found by Slater's criterion is highlighted in red.

a value very close to that predicted in Ref. 12, with a relative error (percent) RE(%) = 2.1%. These results demonstrate the method's effectiveness in accurately identifying the transition point for the destruction of invariant curves, aligning with theoretical expectations and reinforcing its reliability.

To corroborate this, Fig. 5 presents the phase space for  $\varepsilon=0.195\,777\,2$  and p=2 from two perspectives. In Fig. 5(a), a large chaotic sea is visible, with many structures, including the invariant spanning curves, destroyed. Figure 5(b) provides an enlarged view of the upper region, highlighting the near-total destruction of invariant curves. The last remaining curve, identified using Slater's theorem, is marked in red. The analyzed point of this curve was  $(\pi,3.138\,114\,857\,512\,855\,2)$ , with recurrence times  $\Gamma_1=982$ ,  $\Gamma_2=1982$ , and  $\Gamma_3=2964$  (for  $\delta=10^{-3}$ ), satisfying Slater's criterion.

We now extend our analysis to other values of the parameter p in order to verify the validity of the expression for  $\varepsilon_c$ . In Fig. 6(a), we present the phase space for p=3, where again we observe a mixed phase space. Again, we highlight four curves found using Slater's criterion. Table II shows the position of each of them, as well as recurrence times found for each case. Note that it is still possible to observe a large number of invariant curves in the upper part of the phase space, indicating that the  $\varepsilon$  value used is smaller than the critical  $\varepsilon_c$ . Therefore, applying the proposed method, we determined that  $\varepsilon_c=0.0935$  (RE(%)=6.5%), which again is very close to the value predicted by Eq. (10). In Fig. 6(b), an enlargement of the region close to the invariant spanning curves is shown, confirming that for this value of  $\varepsilon$  the vast majority of curves have already been destroyed.

In the same figure, we highlight in red the last invariant spanning curve found using Slater's criterion.

So far, we have applied the method to even and odd values of p, and in both cases it was possible to determine the position of the curves in the phase space, as well as find the critical parameter for the respective value of p. In Fig. 7, we show the results obtained for higher values of p. In this figure, the solid line is given by Eq. (10), while the points represent the numerical results obtained with the proposed method. It is possible to notice the correspondence between the numerical results and the expected value.

In oval billiards, the presence or absence of comprehensive invariant curves marks the transition to chaos, which may not occur in other billiards models.<sup>25</sup> Nevertheless, our method remains a useful tool for analyzing the phase space structure in mixed-chaotic systems. Even when there are no global invariant curves separating chaotic and regular regions, Slater's theorem can still be applied

**TABLE II.** Recurrence times for  $\delta = 10^{-4}$  and coordinates for identified invariant spanning curves in Fig. 6(a).

	$\Gamma_1$	$\Gamma_2$	$\Gamma_3$	$(\theta, \alpha)$
Curve 4	4493	9660	5167	$(\pi, 3.0735)$
Curve 3	2647	5019	2372	$(\pi, 3.0674)$
Curve 2	1269	6277	7546	$(\pi, 3.0299)$
FISC	2510	5499	2989	$(\pi, 3.0105)$

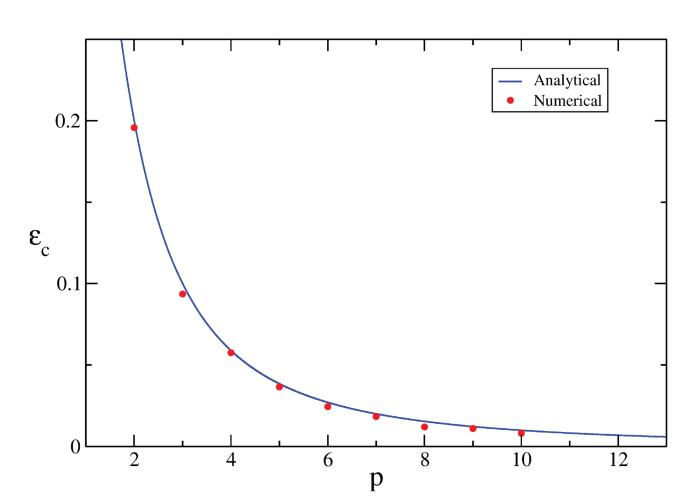


**FIG. 7.** Comparison between the expected  $\varepsilon_c$  result, given by Eq. (10), and the result found using the method based on Salter's theorem.

within islands of stability immersed in the chaotic sea. In such cases, it allows the identification and study of the invariant curves within these isolated islands, providing insights into their rupture and the local transition to chaos. While in this work we have specifically used the method to study invariant spanning curves, it could also be applied to other types of invariant structures, such as islands, further broadening its applicability in the analysis of complex dynamical systems.

#### V. ROTATION NUMBER

An observable that also provides relevant information about invariant spanning curves is the rotation number  $\omega$ . It quantifies the periodic or quasi-periodic behavior of a trajectory around a fixed point or a closed curve in a dynamical system, measuring the average angular displacement per iteration. In other words,  $\omega$  indicates how the phase variable  $\theta$  evolves over time relative to the total number of iterations, capturing the global behavior of an orbit. An orbit  $\{(\theta_t, \alpha_t) : t \in \mathbb{Z}\}$ , has rotation number  $\omega$  if the limit

$$\omega = \lim_{N \to \infty} \frac{1}{N} \sum_{t=0}^{N} \Omega(\theta_t)$$
 (11)

exists.<sup>26</sup> The function  $\Omega(\theta_t)$  defines how the collision angle or trajectory direction changes with each collision. Thus, in Eq. (11),  $\sum_{t=0}^{N} \Omega(\theta_t) = \theta_N - \theta_0$  and N corresponds to the number of iterations.

The rotation number plays a fundamental role in distinguishing different dynamical regimes. When  $\omega$  is a rational number, the trajectory is periodic, meaning the orbit eventually repeats itself after a finite number of iterations. Conversely, if  $\omega$  is irrational, the orbit is quasi-periodic, densely filling a toroidal surface without repeating exactly. In Fig. 8(b), we show the profile of the rotation number  $\omega$ , calculated along the red dashed line in Fig. 8(a). For chaotic regions, the rotation number does not converge, which is represented by the cloud of points in Fig. 8(b). On the other hand, for periodic

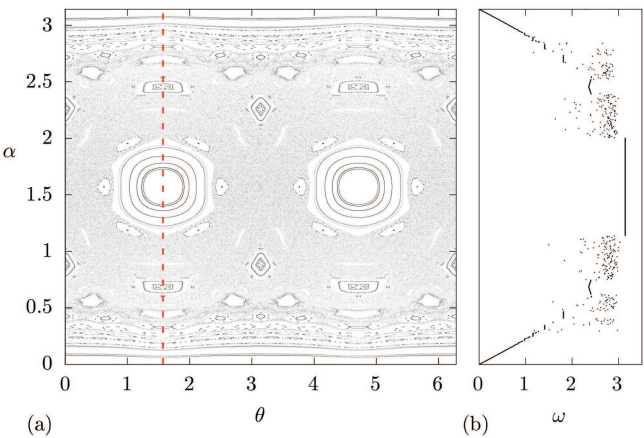


**FIG. 8.** (a) Phase space for  $\varepsilon=0.1$  and p=2. (b) Rotation number profile calculated by the long red dashed line in (a).

or quasi-periodic regions, this number converges, corresponding to the plateaus in Fig. 8(b), highlighting the large chain of islands with a rotation number equal to  $\pi$ . This characterization allows us to detect invariant spanning curves since these curves act as barriers in phase space, preventing global chaos. When an invariant spanning curve exists, the rotation number remains constant along the curve, reinforcing its role as an effective transport barrier in the system.

Regarding the invariant spanning curves, the result presented in Fig. 8(b) shows that the rotation number goes continuously to 0 as  $\alpha$  tends to  $\pi$  (upper part of the phase space) or as  $\alpha$  tends to 0 (lower part phase space). We believe that this behavior occurs due to the fact that  $\omega$  corresponds to the average variation of the  $\theta$  variable and as seen previously, an invariant curve borders the billiard wall, making the distance traveled from one collision to another very small and, consequently, the variation of  $\theta$  is also small. Furthermore, these curves are quasi-periodic and have irrational rotation numbers. The irrational rotation number ensures that the orbit does not repeat exactly, but fills the curve densely.

In addition to the rotation number profile, we constructed the rotation number space shown in Figs. 9 and 10. This space corresponds to a region of the model's phase space, where the color is related to the rotation number. Black and blue colors correspond to rotation number values approximately between 0 and 1, while warm colors such as yellow, orange, and red correspond to values ranging between 2.5 and  $\pi$ . Intermediate values are represented in shades of green.

In Fig. 9, we have a central region highlighted in red, which corresponds to a chain of islands with a rotation number equal to  $\pi$ , evidenced by the largest plateau in Fig. 8(b). Still in Fig. 9, we observe two regions located at the bottom and top edges of the figure, with rotation numbers between 0 and 1, which correspond to the regions where the invariant spanning curves are located. Note that in these regions there is a transition from blue to black, again indicating that the rotation number tends to 0 when  $\alpha \to 0$  (or  $\alpha \to \pi$ ). Finally, between these two regions, we have a large predominantly

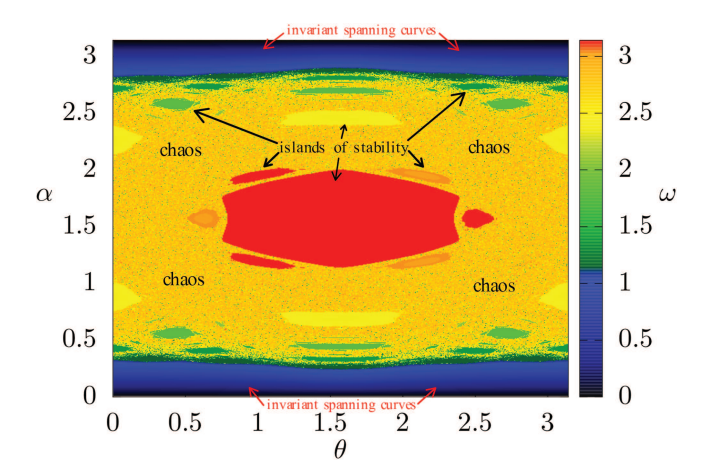


**FIG. 9.** Rotation number space for  $\varepsilon=0.1$  and p=2, the color scale corresponds to the rotation number  $\omega$ . Chaos is in the large predominantly area.

orange area, where there is no convergence of the rotation number, characterizing a chaotic region.

For a more detailed analysis of the border between the blue and green regions, we made an enlargement, as shown in Fig. 10. In this figure, we highlight the first invariant spanning curve, marked in red. Above this curve, we notice a smooth transition from blue to black, reinforcing the presence of other spanning curves and the absence of chaos in this region. On the other hand, below the first invariant spanning curve, it is possible to notice a dense layer where the rotation number is very close to that of the curve, at least for a certain time interval. Further down, it is already possible to notice the presence of islands and chaotic regions, consequently presenting a greater variation in the rotation number.

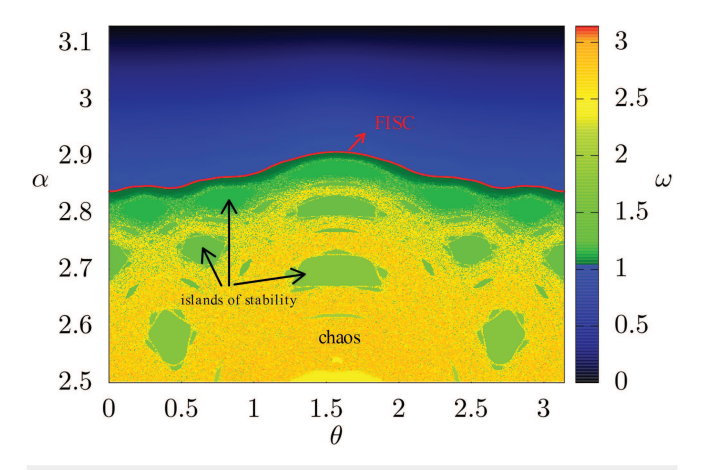


**FIG. 10.** Enlargement of the upper region of the rotation number space in Fig. 9. The First Invariant Spanning Curve (FISC), highlighted in red, highlights its role as a barrier.

#### VI. CONCLUSIONS

In this study, we investigated the dynamic properties of an oval billiard, with emphasis on determining the invariant spanning curves, which delimit regions of chaos in phase space. We use Slater's theorem as a theoretical basis for developing a numerical method capable of accurately locating these curves and determining the critical value of the parameter  $\varepsilon$ , from which the invariant curves are destroyed.

Furthermore, rotation number analysis provided additional information not only about the behavior of the invariant spanning curves but also about the dynamics of the system as a whole. Indicating the transition between periodic and chaotic regions in phase space. The visualization of the rotation number space revealed the influence of invariant spanning curves on the system dynamics and their role as a barrier in the phase space.

The results obtained demonstrate the effectiveness of the proposed method, evidenced by the agreement with the analytical results present in the literature. We identified the invariant spanning curves for different values of the parameter p and verified the validity of the expression for the critical parameter  $\varepsilon_c$ , comparing the theoretical values with those obtained numerically. We believe this is a robust tool for finding invariant curves and determining critical parameters.

#### **ACKNOWLEDGMENTS**

We would like to acknowledge financial support from the Brazilian agencies: São Paulo Research Foundation (FAPESP)—Grant No. 2018/03211-6 and CNPq—Grant No. 30416/2021-4. J.D.V.H. thanks Federal Institute of Education, Science and Technology of South of Minas Gerais—IFSULDEMINAS. M.H. is funded by national funds through the FCT—Fundação para a Ciência e a Tecnologia, I.P., under the scope of the projects UIDB/00297/2020 (https://doi.org/10.54499/UIDB/00297/2020) and UIDP/00297/2020 (https://doi.org/10.54499/UIDP/002 97/2020) (Center for Mathematics and Applications).

# **AUTHOR DECLARATIONS**

# Conflict of Interest

The authors have no conflicts to disclose.

### **Author Contributions**

Joelson D. V. Hermes: Conceptualization (equal); Data curation (equal); Formal analysis (equal); Funding acquisition (equal); Investigation (equal); Methodology (equal); Project administration (equal); Resources (equal); Software (equal); Validation (equal); Visualization (equal); Writing – original draft (equal); Writing – review & editing (equal). Matheus Hansen: Conceptualization (equal); Data curation (equal); Formal analysis (equal); Funding acquisition (equal); Investigation (equal); Methodology (equal); Software (equal); Validation (equal); Visualization (equal); Writing – original draft (equal); Writing – review & editing (equal). Sishu S. Muni: Conceptualization (equal); Data curation (equal); Formal analysis (equal); Funding acquisition (equal); Investigation (equal); Methodology (equal); Validation (equal);

Visualization (equal); Writing – original draft (equal); Writing – review & editing (equal). **Edson D. Leonel:** Conceptualization (equal); Data curation (equal); Formal analysis (equal); Funding acquisition (equal); Investigation (equal); Methodology (equal); Supervision (equal); Validation (equal); Visualization (equal); Writing – original draft (equal); Writing – review & editing (equal). **Iberê Luiz Caldas:** Conceptualization (equal); Data curation (equal); Formal analysis (equal); Funding acquisition (equal); Investigation (equal); Methodology (equal); Project administration (equal); Resources (equal); Software (equal); Supervision (equal); Validation (equal); Visualization (equal); Writing – original draft (equal); Writing – review & editing (equal).

#### **DATA AVAILABILITY**

The data that support the findings of this study are available from the corresponding author upon reasonable request.

#### REFERENCES

- $^{\rm 1}$  N. Chernov and R. Markarian, Chaotic Billiards (American Mathematical Society, 2023), Vol. 127.
- <sup>2</sup>S. Tabachnikov, *Geometry and billiards*, vol. 30 of student mathematical library (American Mathematical Society, Providence, RI, 2005), Vol. 28, pp.59–70.
- <sup>3</sup>D. Sweet, B. W. Zeff, E. Ott, and D. P. Lathrop, "Three-dimensional optical billiard chaotic scattering," Physica D 154, 207–218 (2001).
   <sup>4</sup>E. Persson, I. Rotter, H.-J. Stöckmann, and M. Barth, "Observation of resonance
- <sup>4</sup>E. Persson, I. Rotter, H.-J. Stöckmann, and M. Barth, "Observation of resonance trapping in an open microwave cavity," Phys. Rev. Lett. **85**, 2478 (2000).
- <sup>5</sup>H.-D. Gräf, H. Harney, H. Lengeler, C. Lewenkopf, C. Rangacharyulu, A. Richter, P. Schardt, and H. Weidenmüller, "Distribution of eigenmodes in a superconducting stadium billiard with chaotic dynamics," Phys. Rev. Lett. 69, 1296 (1992).
- <sup>6</sup>C. Marcus, A. Rimberg, R. Westervelt, P. Hopkins, and A. Gossard, "Conductance fluctuations and chaotic scattering in ballistic microstructures," Phys. Rev. Lett. **69**, 506 (1992).
- <sup>7</sup>J. Möser, "On invariant curves of area-preserving mappings of an annulus," Nachr. Akad. Wiss. Göttingen, II 1, 1–20 (1962).
- <sup>8</sup>J. Meiss, "Symplectic maps, variational principles, and transport," Rev. Mod. Phys. **64**, 795 (1992).
- <sup>9</sup>E. D. Leonel, J. A. De Oliveira, and F. Saif, "Critical exponents for a transition from integrability to non-integrability via localization of invariant tori in the Hamiltonian system," J. Phys. A: Math. Theor. 44, 302001 (2011).

- <sup>10</sup>M. Mugnaine, I. Caldas, J. Szezech, Jr., R. Viana, and P. Morrison, "Shearless effective barriers to chaotic transport induced by even twin islands in nontwist systems," Phys. Rev. E **110**, 044201 (2024).
- systems," Phys. Rev. E 110, 044201 (2024).

  11 A. Celletti, "Some KAM applications to celestial mechanics," Discrete Contin.

  Dvn. Syst.-S 3, 533–544 (2010).
- <sup>12</sup>D. F. Oliveira and E. D. Leonel, "On the dynamical properties of an elliptical-oval billiard with static boundary," Commun. Nonlinear Sci. Numer. Simul. 15, 1092-1102 (2010).
- <sup>13</sup>N. B. Slater, "The distribution of the integers n for which  $\{\theta n\} < \varphi$ ," in *Mathematical Proceedings of the Cambridge Philosophical Society* (Cambridge University Press, 1950), Vol. 46, pp. 525–534.
- $^{14}$ N. B. Slater, "Gaps and steps for the sequence  $n\theta \mod 1$ ," in *Mathematical Proceedings of the Cambridge Philosophical Society* (Cambridge University Press, 1967), Vol. 63, pp. 1115–1123.
- <sup>15</sup>F. Lenz, F. K. Diakonos, and P. Schmelcher, "Tunable Fermi acceleration in the driven elliptical billiard," Phys. Rev. Lett. 100, 014103 (2008).
- <sup>16</sup>L. A. Bunimovich, "On ergodic properties of certain billiards," Funct. Anal. Appl. 8, 254–255 (1974).
- <sup>17</sup>D. F. M. Oliveira, J. Vollmer, and E. D. Leonel, "Fermi acceleration and its suppression in a time-dependent Lorentz gas," Physica D 240, 389–396 (2011).
- <sup>18</sup>M. Hansen, R. Egydio de Carvalho, and E. D. Leonel, "Influence of stability islands in the recurrence of particles in a static oval billiard with holes," Phys. Lett. A 380, 3634–3639 (2016).
- <sup>19</sup>V. Lopac, I. Mrkonjic, N. Pavin, and D. Radic, "Chaotic dynamics of the elliptical stadium billiard in the full parameter space," Physica D **21**7, 88–101 (2006).
- <sup>20</sup>E. D. Leonel and C. P. Detmann, "Recurrence of particles in static and time varying oval billiards," Phys. Lett. A **376**, 1669–1674 (2012).
- <sup>21</sup> M. Hansen, D. R. da Costa, I. L. Caldas, and E. D. Leonel, "Statistical properties for an open oval billiard: An investigation of the escaping basins," Chaos Solitons Fractals **106**, 355–362 (2018).
- <sup>22</sup>C. V. Abud and I. L. Caldas, "On Slater's criterion for the breakup of invariant curves," Physica D 308, 34–39 (2015).
   <sup>23</sup>J. D. Hermes, M. A. dos Reis, I. L. Caldas, and E. D. Leonel, "Break-up of
- <sup>23</sup>J. D. Hermes, M. A. dos Reis, I. L. Caldas, and E. D. Leonel, "Break-up of invariant curves in the Fermi-Ulam model," Chaos Solitons Fractals **162**, 112410 (2022).
- <sup>24</sup>Y. H. Huggler, J. D. Hermes, and E. D. Leonel, "Application of the Slater criteria to localize invariant tori in Hamiltonian mappings," Chaos **32**, 093125 (2022).
- <sup>25</sup>M. Hansen, D. R. da Costa, I. L. Caldas, and E. D. Leonel, "Statistical properties for an open oval billiard: An investigation of the escaping basins," Chaos Solitons Fractals **106**, 355–362 (2018).
- <sup>26</sup>E. Sander and J. Meiss, "Birkhoff averages and rotational invariant circles for area-preserving maps," Physica D **411**, 132569 (2020).